Colloid Polym Sci 277:709–718 (1999)

ORIGINAL CONTRIBUTION

Tz. Ivanova
N. Grozev
I. Panaiotov
J.E. Proust

Role of the molecular weight and the composition on the hydrolysis kinetics of monolayers of poly(α-hydroxy acid)s

Received: 7 December 1998
Accepted in revised form: 8 March 1999

Tz. Ivanova · N. Grozev · I. Panaiotov (✉)
Biophysical Chemistry Laboratory
University of Sofia
J. Bourchier Str. 1
1126 Sofia, Bulgaria

J.E. Proust
Pharmacie Galénique et Biophysique
Pharmaceutique
Faculté de Pharmacie
16 Bd Daviers
F-49100 Angers, France

Abstract The hydrolysis kinetics of spread insoluble monolayers of poly(α-hydroxy acid)s with various molecular weights and lactic acid–glycolic acid molar ratios was followed by measuring simultaneously the decrease in the surface area at constant surface pressure and the evolution of the surface potential. The interfacial hydrolysis at alkaline pH leads to the progressive fragmentation of the polymer molecules and the appearance of charged insoluble products (detected by measuring the surface potential) and small soluble fragments (detected by measuring the decrease in the surface area). The data obtained by both approaches were interpreted in the framework of the random scission model. The rates of hydrolysis are larger for polymers with smaller initial polymerization numbers and increase with the decrease in the molar ratio of lactic acid units.

Key words Basic hydrolysis · Monolayer · Poly(α-hydroxy acid)s

Introduction

The homo- and copolymers of lactic and glycolic acids were among the first biodegradable materials used for the design of controlled delivery systems [1–3]. In vivo, the erosion of the polymer matrix of the microparticles controls the release of the incorporated drug. The role of the various degradation factors and the mechanism of erosion of biodegrading microparticles have been investigated intensively [1–14]. A contribution of prime importance to the complex degradation process is the hydrolysis and scission of ester bonds of the polymer and the progressive appearance of water-soluble oligomers. Depending on the method of formation, the microparticles may contain a certain number of small or relatively large pores. The hydrolytic reaction is localized at the polymer–water internal surfaces of the pores as well as at the external surface of the microparticle. The chemical reaction is coupled with various interfacial phenomena such as mass transfer of the reactant products, interfacial accumulation of charged hydrolytic insoluble products, desorption and solubilization of small oligomers and so on.

In order to analyse the interfacial organization of the hydrolysis, a simple model system has recently been proposed – a poly(D,L-lactide) monolayer spread on a basic or an acidic aqueous subphase [15, 16]. The advantage of the monolayer approach is the ability to control the interfacial organization of the ester groups and to realize the optimum conditions for hydrolysis, when all ester bonds are accessible to the underlying aqueous subphase containing OH^- and H^+. The course of the interfacial hydrolysis at alkaline and acidic pH, leading to the appearance of charged insoluble and water–soluble fragments, can be easily followed for 1 h or more by using a traditional barostat surface balance [15, 16]. A theoretical approach based on the random fragmentation of polymer molecules was proposed and compared with the experimental data for the decrease in area and surface potential at constant surface pressure for a poly(D,L-lactide) monolayer (PLA50).

The purpose of this paper is to study the role of the molecular weight and the chemical composition (lactic acid–glycolic acid ratio) of the polymer on the interfacial hydrolysis at alkaline pH.

Materials and methods

Materials

The following polymers were used (Fig. 1). Two poly(**D**,**L**-lactide) stereocopolymers (PLA50) were obtained from CRBPA (Montpellier, France) and Boehringer Ingelheim (Paris, France). The molecular weights (M_w) determined by size-exclusion chromatography and the polymolecularity index (I) were M_w = 41 600 (I = 1.6) and M_w = 124 400 (I = 2.3), respectively.

Three poly(**D**,**L**-lactide-*co*-glycolide) stereocopolymers were supplied by Boehringer Ingelheim (Paris, France): PLA42.5GA15 with M_w = 87 000 (I = 1.6); PLA25GA50 with M_w = 14 300 (I = 2.3) and M_w = 102 900 (I = 2.3), respectively.

Na_2HPO_4, HCl and dichloromethane (DCM) were supplied by Prolabo (Paris, France) and NaOH was purchased from Merck (Darmstadt, Germany). Doubly distilled water was used.

Measurements at the air–water interface

The monolayers of poly(α-hydroxy acid)s were spread from a volatile DCM solution (c = 1 gdm^{-3}) using an Exmire microsyringe on the aqueous subphases at pH 11.4 (a buffer solution comprising 2.5×10^{-2} M Na_2HPO_4 and 0.91×10^{-2} M NaOH). DCM was found to be a good solvent leading to a deployment of polymer chains and the formation of a more unfolded structure at the air–water interface [17].

The surface pressure (π) was measured using a KSV-2200 (Finland) surface balance with a platinum plate. The surface potential (ΔV) was measured simultaneously by using a gold-coated ^{241}Am ionizing electrode, a reference electrode and a KP 511 (Kriona, Bulgaria) electrometer, connected to a PC provided with user software for real-time data measurement. As usual, the surface potential of the pure aqueous surface fluctuated for about 30 min. The surface potential then became constant and spreading of the monolayer could be performed. The accuracy of the initial surface potential value was ±15 mV; however, the accuracy of the rate of surface potential variation dΔV/dt was 1 mV s^{-1}.

Two kinds of experiments were performed:

1. Surface pressure–area and surface potential–area isotherms were obtained after spreading the polyesters from DCM solution on the aqueous subphase at neutral pH on the maximum available area of the KSV-2200 surface balance. The values of the surface pressure after spreading were less than 0.1 mN m^{-1}. The monolayers were then compressed with constant velocity U_b = 10 cm^2 min^{-1}.
2. The decrease (ΔA) in the surface area and the surface potential (ΔV) as a function of time were measured simultaneously during the basic hydrolysis of the polyester monolayers at constant surface pressure by using an automatic barostat KSV-2200 surface balance. A "zero-order" trough, composed of a reaction compartment (area 50 cm^2, volume 50 cm^3) and a reservoir compartment (area 270 cm^2), communicating by means of a narrow surface channel (width 0.5 cm), was used (Fig. 2). After spreading over the maximum available area (320 cm^2) of the KSV-2200 surface balance, the polyester monolayers were compressed with constant velocity (U_b = 100 cm^2 min^{-1}) until a given value of the surface pressure was attained and the barostat setup was switch on. The water subphase at pH 11.4 in the reaction compartment was stirred continuously with a magnetic rod at 250 rpm. The water subphase in the reservoir compartment was maintained at neutral pH.

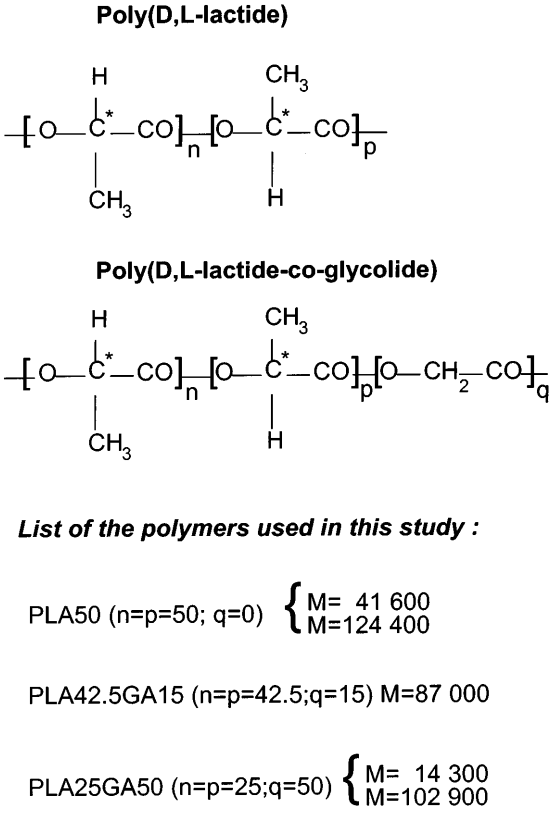

Fig. 1 Chemical formulae of poly(α-hydroxy acid)s

Molecular models

Molecular models were created by using the PCMODEL software (Serena Software 1993). The force field used in PCMODEL is derived from the MM2 (QCPE 395, 1977) force field of N.L. Allinger with the p-VESCF routines taken from MMP1 (QCPE 318). The program gives the structure of the monomer units. The monomers are situated at the air–water interface taking into account their hydrophilic–hydrophobic balance.

Theoretical model

The scheme and the products of hydrolysis in highly basic aqueous media in the well–known case of the monoester are presented in Fig. 3. At each hydrolytic step a net negative charge situated at the end of the polymer fragment appears (one charge per fragment). The following equation describes the interfacial hydrolysis of the polyester at alkaline pH.

$$-\frac{ds}{dt} = kc_{OH^-}s(t) \quad , \tag{1}$$

where k is the rate constant, c_{OH^-} is the concentration of hydroxyl ions at the level of the chemical interaction and $s(t)$ is the number of intact ester groups per square centimetre at time t.

The electric field of a charged monolayer alters the concentration of soluble ions in the region immediately below the film. As a result of the progressive accumu-

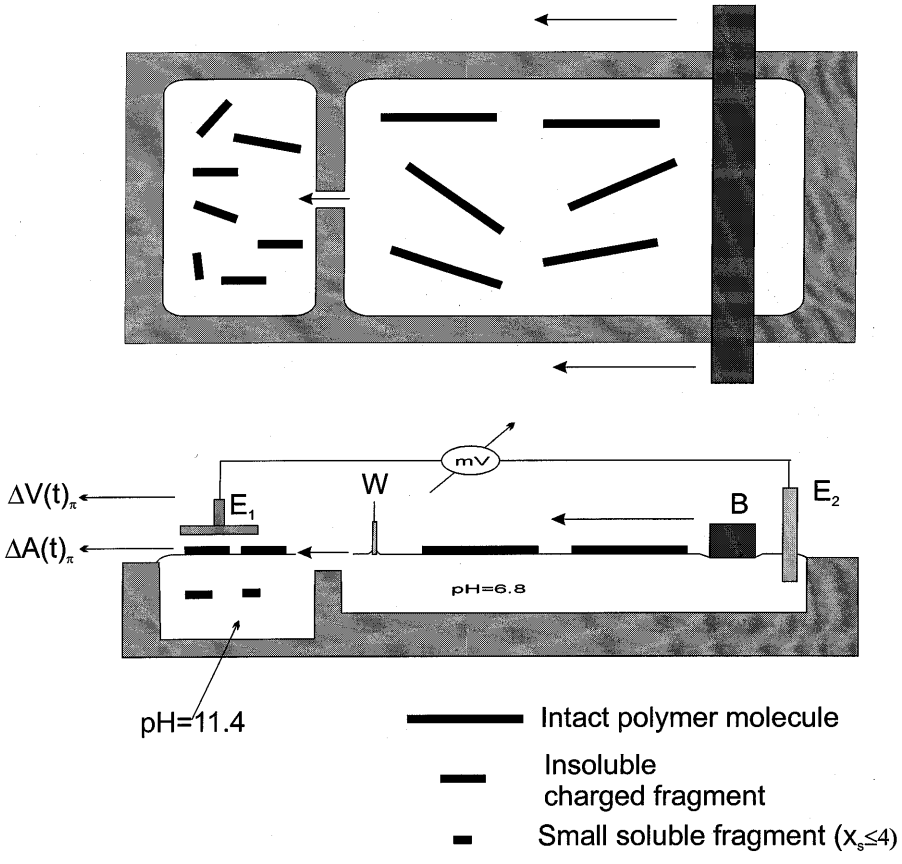

Fig. 2 Scheme of the "zero order" trough used for measurements during interfacial hydrolysis. The trough is composed of a reaction compartment (volume 50 cm^3, surface area 50 cm^2) and a reservoir compartment (270 cm^2) communicating by means of a narrow surface channel (width 0.5 cm). *B* – barrier; *W* – Wilhelmy plate; E_1 – ionizing electrode; E_2 – reference electrode

lation of negatively charged hydrolytic products, the concentration of hydroxyl ions (c_{OH^-}) at the level of the chemical reaction becomes less than in the bulk phase ($c^b_{OH^-}$) in accordance with the Boltzmann equation

$$c_{OH^-} = c^b_{OH^-} \exp\left(-\frac{e_0\psi}{kT}\right) , \quad (2)$$

where ψ is the electrostatic potential at the level of the reaction, e_0 is the electrostatic charge, k is the Boltzmann constant and T is the absolute temperature.

In order to estimate the concentration of hydroxyl ions really involved in the chemical reaction, we prefer to use Eq. (2) in the following form:

$$c_{OH^-} = c^b_{OH^-} \exp\left(-\frac{\lambda e_0\psi_0}{kT}\right) , \quad (3)$$

where ψ_0 is the electrostatic potential in the plane of the interface relative to the subjacent aqueous phase con-

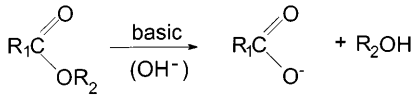

Fig. 3 Scheme of the catalytic hydrolysis of a monoester in highly basic aqueous media

taining monovalent counterions and λ is a parameter taking into account the local energy of electrostatic repulsion at the level of the chemical interaction.

The most frequently used expression for ψ_0 is based on the Gouy–Chapman classical theory of the diffuse double layer.

$$\psi_0 = \frac{2kT}{e_0} \sinh^{-1}\left(\frac{\sigma}{(2n_i\varepsilon kT/\pi)^{1/2}}\right) \quad (4)$$

and

$$\psi = \psi_0 e^{-\chi z} , \quad (5)$$

where σ is the charge per square centimetre of a plane, impenetrable, uniformly charged surface; n_i is the concentration of the monovalent counterions in the bulk solution, presented as point charges being able to approach right up to the plane of the charges at $z = 0$, ε is the dielectric constant of water, z is the distance from the plane charged surface and $\chi^{-1} = \left(\frac{8\pi e_0^2}{\varepsilon kT} n_i\right)^{-1/2}$ is the Debye distance. The value of ψ_0 can be obtained experimentally from the data for ΔV. According to Schulman and Rideal [18] the surface potential for a charged monolayer is determined by the contributions of the dipole moments and of the double layer of the counterions:

$$\Delta V = 4\pi\mu_{\perp}\Gamma + \psi_0 \ , \tag{6}$$

where $\mu_{\perp} \equiv \frac{\mu}{\varepsilon'}$, is the sum of vertical components of the dipole moments in one monomer, ε' is the dielectric constant in the plane of the monolayer and Γ is the surface density of α-hydroxy acid units, which remains constant during hydrolysis under barostatic conditions ($\Gamma = \Gamma_0$). The initial value of ΔV at $t = 0$ before the appearance of charged units, is given by

$$\Delta V_0 = 4\pi\mu_{\perp}\Gamma_0 \tag{7}$$

Assuming that the contribution of the dipoles to ΔV of the monolayer, given by the first term on the right side of Eq. (6), is independent of the contribution of the double layer, ψ_0 is given by $\Delta V_0 - \Delta V(t)$ (see also Results and discussion).

The parameter λ introduced by Eq. (3) can be calculated in the framework of the Gouy–Chapman ideal system. If the reaction occurs at the geometrical plane surface ($z = 0$) or at the Debye distance ($z = \chi^{-1}$), λ takes the value of 1 or 0.368, respectively, in the absence of surface charge $\lambda = 0$. Finally, λ can be used as a fitting parameter to describe more precisely the role of the electrical factor on interfacial hydrolysis (see also Results and discussion).

From Eqs. (1) and (3) we obtain the following kinetics equation describing the interfacial hydrolysis ($k_0 = kc^{b}_{OH^-}$):

$$-\frac{\mathrm{d}s}{\mathrm{d}t} = k_0 \exp\left(-\frac{\lambda e_0 \psi_0}{kT}\right) s \ . \tag{8}$$

Thus, the degree of completion, α, of the hydrolysis (the fraction of the broken ester bonds) is given by the following expression

$$\alpha(t) = 1 - \frac{s}{s_0} = 1 - \exp\left[-k_0 \int_0^t \exp\left(-\frac{\lambda e_0 \psi_0}{kT}\right)\mathrm{d}t\right] \ , \tag{9}$$

where s_0 is the initial number of intact ester groups at time $t = 0$.

Eq. (8) must be combined with an equation describing the process of uniform random fragmentation of the linear polyester molecules. With the assumption that the reaction activities of all ester groups are equivalent, the number ω_x of segments constituted by x units (obtained during the fragmentation of one polymer molecule with initial polymerization number $n_p \equiv s_0 + 1$) is given by

$$\omega_x(\alpha) = \alpha(1-\alpha)^{x-1}[2 + (s_0 - x)\alpha] \ . \tag{10}$$

The fragmentation process leads to the formation of large insoluble negatively charged fragments and small soluble ones, constituted by $x \le x_s$ units. The fraction β of the solubilized α-hydroxy acid units per polymer molecule can be easily obtained from Eq. (10).

$$\beta(\alpha) = \frac{\sum_{x=1}^{x_s} \omega_x x}{s_0} \tag{11}$$

The fraction, γ, of the charges situated at the ends of the insoluble fragments remaining at the interface with respect to all the ester bonds, s_0, per polymer molecule with initial polymerization number $n_p \equiv s_0 + 1$, can also be calculated from eq. (10).

$$\gamma(\alpha) = \frac{s_0\alpha - \sum_{x=1}^{x_s} \omega_x}{s_0} \ . \tag{12}$$

Two forms of the continuity equation of mass conservation at the interface must be associated with Eqs. (9) and (11) and with Eqs. (9) and (12), respectively. These equations are deduced numerically from the experimental results for $\Delta A(t)$, obtained under barostatic conditions. Taking into account the progressive solubilization of polymer molecules initially present in the reaction compartment ($A_0 = 50\ \mathrm{cm}^2$) as well as the contribution of the i portions ($\Delta A_{t=t_i}$) of intact polymer molecules supplied progressively by the reservoir to the reaction compartment (see Fig. 2), the following theoretical expressions for the surface area decrease, $\Delta A(t)$, and the number of charged lactic acid units per square centimetre, $s^-(t)$, during hydrolysis are obtained

$$\Delta A(t) = A_0\,\beta(t) + \sum_{i=0}^{i} \Delta A(t_i)\,\beta(t - t_i) \tag{13}$$

$$s^-(t) = \frac{\Gamma_0}{A_0}\left[A_0\,\gamma(t) + \sum_{i=0}^{i} \Delta A(t_i)\,\gamma(t - t_i)\right] \ . \tag{14}$$

Results and discussion

State of the monolayers of poly(α-hydroxy acid)s spread at neutral pH

The surface pressure area and surface potential area isotherms for all polymers studied, spread at neutral pH were measured. As an example, the isotherms $\pi(A)$ (curve 1) and $\Delta V(A)$ (curve 2) obtained for the PLA50 ($M_w = 124\,400$) monolayer are presented in Fig. 4. The inflection point observed at $\pi = 9\ \mathrm{mN\ m^{-1}}$ and $A \sim 17\ \mathrm{Å}^2$ per monomer in the $\pi(A)$ isotherm corresponds to a saturation in the $\Delta V(A)$ isotherm and a close packing of all lactic acid units at the interface [19]. By using the Helmholtz equation (Eq. 7) with $\Delta V = 440$ mV, $\Gamma = 5.55 \times 10^{14}$ monomers cm^{-2} and typical value of $\varepsilon' = 2$ for the polyethylene chains, a value of $\mu = 420$ mD for the monomer is obtained.

Figure 5 gives the probable interfacial disposition of a part of the PLA50 molecule with three lactic acid units in which the main-chain backbone tends to orient so that the polar parts (the carbonyl groups) interact predominantly with the aqueous phase while the non-polar ones (the methyl groups) interact with the

nonaqueous phase. The value of $A \sim 17\,\text{Å}^2$ per monomer is in agreement with the linear dimension $\ell = 4.13$ Å of one lactic acid unit ($\ell^2 \approx 17\ \text{Å}^2$). The experimental value of $\mu = 420$ mD argues in favour of the idea that the most important contribution in the effective dipole moment is due to the dipole moment of 360 mD [18] of a carbonyl group anchored to the aqueous phase.

The phase transition observed at further compression was interpreted [20–22] as the formation into the adjacent air phase of 3D structures (loops) organized in microdomains.

The $\pi(A)$ isotherms for all the polymers studied are presented in Fig. 6. The coordinates of the inflection point corresponding to the close packing of the units depends on the molecular weight and mainly on the lactic acid–glycolic acid molar ratio $X_{LA/GA}$ [e.g. $\pi = 9\,\text{mN m}^{-1}$ and $A \sim 17\,\text{Å}^2$ for $X_{LA/GA} = 1$ ($M_w = 124\,400$); $\pi \sim 7.5\,\text{mN m}^{-1}$ and $A \sim 17\,\text{Å}^2$ for $X_{LA/GA} = 0.85$ ($M_w = 87\,000$); $\pi \sim 6.2\,\text{mN m}^{-1}$ and $A \sim 12\,\text{Å}^2$ for $X_{LA/GA} = 0.50$ ($M_w = 14\,300$); $\pi \sim 6\,\text{mN m}^{-1}$ and $A \sim 11\,\text{Å}^2$ for $X_{LA/GA} = 0.50$ ($M_w = 102\,900$)]. The observed values of area per unit are in accordance with the molecular models with corresponding chemical composition (data not shown).

The shape of the transition (2D → 3D) also depends on the chemical composition of the polymers and on the lactic acid–glycolic acid molar ratio. A longer plateau is observed for monolayers with a higher percentage of lactic acid. This observation is related to the stronger hydrophobic interactions between the lactic acid units at the interface due to the presence of the methyl group.

Hydrolysis kinetics at alkaline pH

The decrease in the area and the change in the surface potential for all polyester monolayers studied were

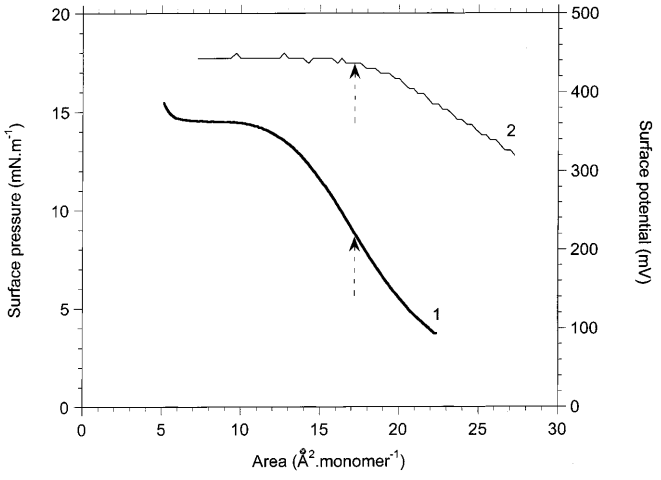

Fig. 4 Surface pressure π (*curve 1*) and surface potential ΔV (*curve 2*) against area A isotherms for a PLA50 ($M_w = 124\,400$) monolayer spread at neutral pH

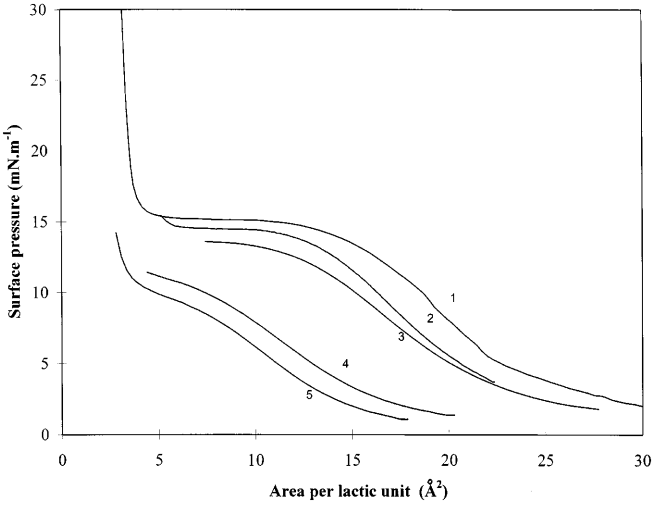

Fig. 6 Surface pressure π–area A isotherms for monolayers of poly(α-hydroxy acid)s spread at neutral pH: *curve 1* - PLA50 ($M_w = 41\,600$); *curve 2* - PLA50 ($M_w = 124\,400$); *curve 3* - PLA42.5GA15 ($M_w = 87\,000$); *curve 4* - PLA25GA50 ($M_w = 14\,300$); *curve 5* - PLA25GA50 ($M_w = 102\,900$)

Fig. 5 Interfacial orientation of a part of the PLA50 molecules with three lactic acid units

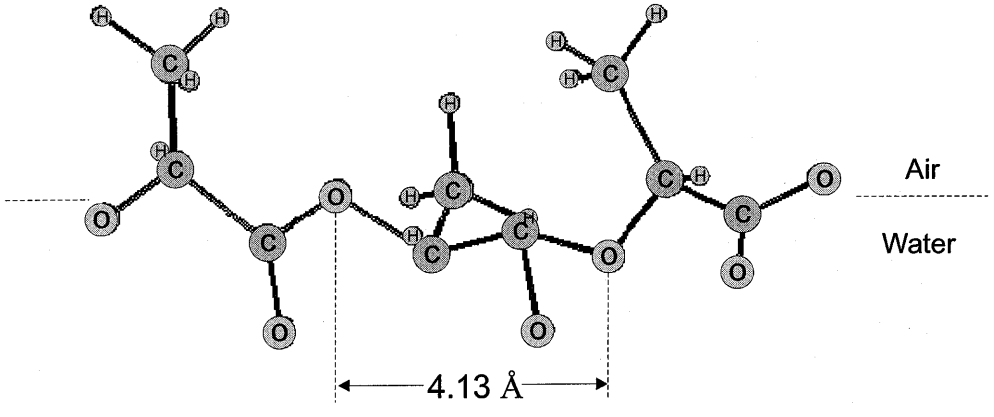

recorded simultaneously during interfacial hydrolysis at various constant surface pressures. As an example, the kinetics of $\Delta A(t)$ (panel A) and $\Delta V(t)$ for the PLA42.5-GA15 (M_w = 87 000) monolayer are presented in Fig. 7. It should be noted that the maximum effect is observed at π = 5 mN m^{-1}, corresponding approximately to the inflection point in the $\pi(A)$ isotherm (Fig. 5) when the number of ester bonds per unit area in contact with the aqueous subphase containing OH^- ions is a maximum.

The observed decrease in area is due to the appearance of small soluble oligomers during the fragmentation of polymer molecules and their instantaneous solubilization in the aqueous subphase. Using an appropriate numerical procedure the predictions of Eq. (13) together with Eqs. (9)–(11) are fitted to the $\Delta A(t)$ curve with one chemical (k_0) or two chemical (k_0 and λ) fitting parameters. As an example, in Fig. 8 the predictions of Eq. (13) for the PLA50 (M_w = 124 400) monolayer at π = 5 mN m^{-1} obtained with one fitting parameter k_0 and the values $\lambda = 0$, $\lambda = e^{-1}$ ($z = \chi^{-1}$) and $\lambda = 1$ based on the Gouy–Chapman classical approach (points) are compared with the experimental data (curve). The prediction obtained with $\lambda = 1$ based on the idea that the reaction occurs at the plane interface at $z = 0$ in the framework of Gouy–Chapman theory is not in agreement with the experimental curve, while the prediction with $\lambda = 0.368$ at $z = \chi^{-1}$ describes the data better. This result seems reasonable because the Debye distance χ^{-1} (32 Å) is comparable with the length of several lactic acid units and the organization of the reaction in the geometrical plane at $z = 0$ seems unrealistic. Note that the comparison based on the Gouy–Chapman ideal system must be considered to be just an estimation because many factors (the nonzero sizes of the reactants and counterions, the decrease in the dielectric constant of water near the surface, etc.) are not considered. In many systems a fortunate compensation of these factors occurs, but such cancellation of errors cannot be general [18, p.79]. That is why, we prefer to fit the experimental data with the parameter $\lambda(t)$. The prediction obtained with two fitting parameters k_0 and λ (triangles) describes the experimental curve of $\Delta A(t)$ better. A sharp step of $\lambda(t)$ from 0 to 1 is observed (Fig. 9).

Similar results are obtained for all the polyester monolayers studied. The decrease in the area with time during hydrolysis at a surface pressure of 5 mN m^{-1} for the five polyester monolayers is presented in Fig. 10 (curves). The theoretical prediction with two fitting parameters k_0 and λ (triangles) describes well the experimental data for $\Delta A(t)$ (curves). The values for the hydrolytic rate constant as a function of the surface pressure are presented in Table 1.

The true chemical rate constants are obtained at the surface pressure where all ester bonds are in the optimum condition to be hydrolyzed and their number

Fig. 7 Decrease in **A** the surface area and in **B** the surface potential with time for a PLA42.5GA15 (M_w = 87 000) monolayer at pH 11.4 and at various constant surface pressures

is a maximum. As already discussed, the optimum surface pressure depends on the molar ratio $X_{LA/GA}$. The reasonable value of π = 5 mN m^{-1} was chosen to compare the hydrolytic rate of all the polyesters studied. The results obtained at 5 mN m^{-1} show that the rate of hydrolysis increases with the decrease in the molar ratio of lactic acid units $X_{LA/GA}$ (from PLA50 to PLA42.5GA15 to PLA25GA50). This observation confirms the usual ideas about the role of the methyl group in the reactivity of lactic acid in comparison with glycolic acid units [23]. As far as the dependence of the rate constants on the molecular weight is concerned, the rate constants obtained are larger for polymers with lower initial molecular weights and polymerization numbers. This result may be related to the usual assumption that the reaction activities of all ester groups are equivalent in the so-called random scission model. In fact, the rate constant at the ends of each chain may be larger than the rate constant inward from the end [13, 14] and the rate constants obtained can be considered as the effective ones. The percentage of end bonds for short-chain polymers (low molecular weight) is larger in comparison with long-chain polymers (high molecular weight) and the apparent rate constant is larger.

On the other hand, the interfacial accumulation of negatively charged products $s^-(t)$ during hydrolysis can be obtained by two independent methods. The first one is the mechanical approach, based on the $\Delta A(t)_{\pi = \text{const}}$ measurement and the analysis of the fragmentation and solubilization processes (Eq. 14). The second approach is based on direct electrical measurement $\Delta V(t)_{\pi = \text{const}}$ and classical interpretation of the surface-potential data (Eq. 6) as the sum of a positive contribution to the dipole moment of the carbonyl group and the negative contribution of the double layer of Na^+ counterions. Assuming that the appearance of negatively charged α-hydroxy acid units does not modify the dipole moment of the carbonyl group, and using the Gouy–Chapman Eq. (4), Eq. (6) becomes

$$\Delta V = 4\pi\mu_\perp\Gamma_0 - \frac{2kT}{e_0}\sinh^{-1}\left[\frac{\sigma}{(2n_+\varepsilon kT/\pi)^{1/2}}\right], \quad (15)$$

where n_+ is the concentration of monovalent Na^+ counterions.

From Eqs. (7) and (15), the corresponding Graham equation is given by

$$s^-(t) = \frac{1}{e_0}\sqrt{\frac{2n_+\varepsilon kT}{\pi}}\sinh\frac{e_0[\Delta V_0 - \Delta V(t)]}{2kT}. \quad (16)$$

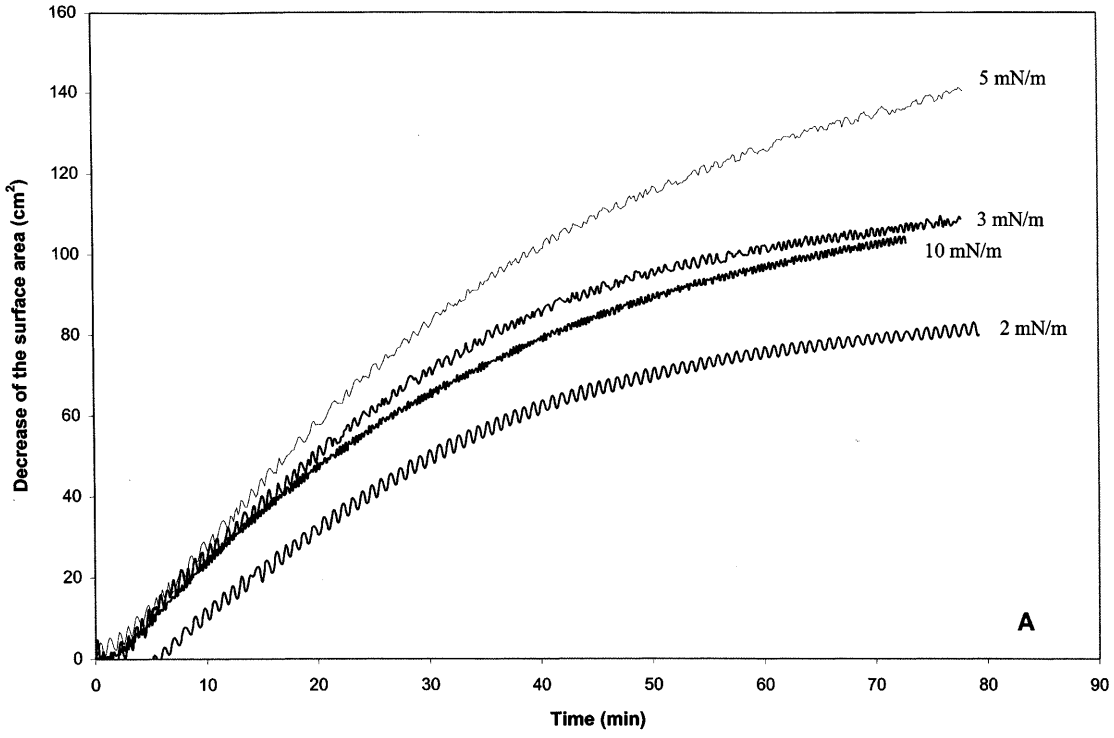

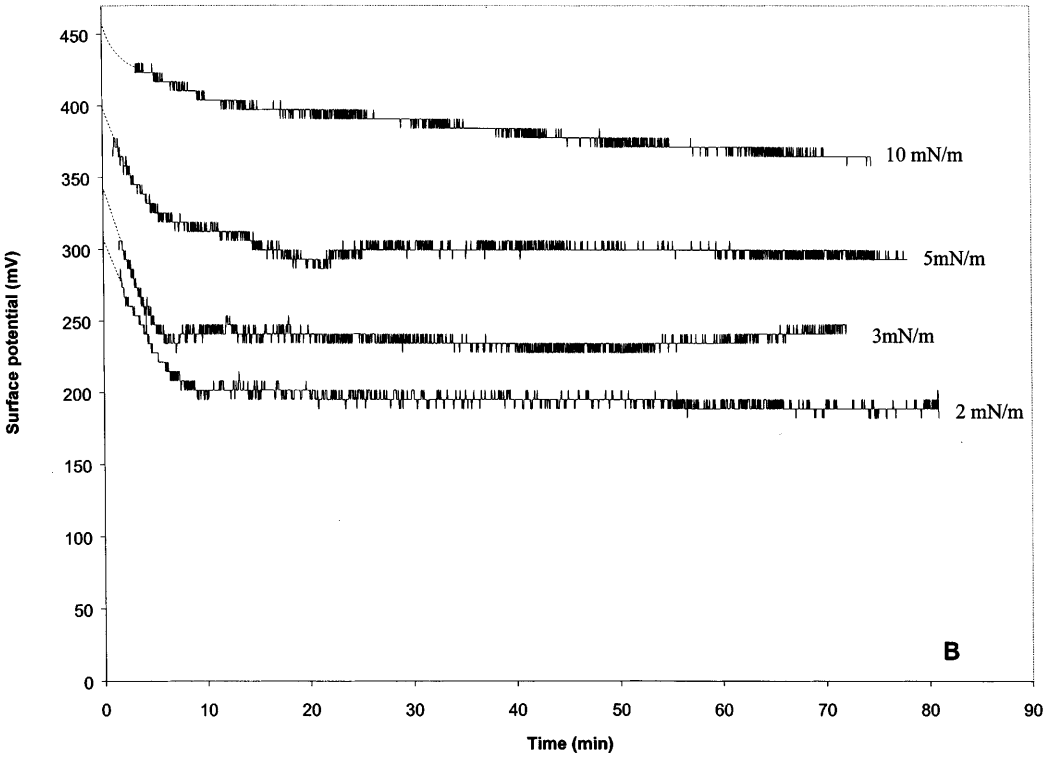

In the more realistic situation when the negative charge modifies the positive dipole moment of the corresponding carbonyl group from $\mu_\perp$ to $\mu'_\perp$ (Fig. 11), the evolution of ΔV with time is described by the following expression:

$$\Delta V = 4\pi\mu_\perp(\Gamma_0 - s^-) + 4\pi\mu'_\perp s^- - \frac{2kT}{e_0}\sinh^{-1}\left(\frac{e_0 s^-}{(2n_+\varepsilon kT/\pi)^{1/2}}\right) . \quad (17)$$

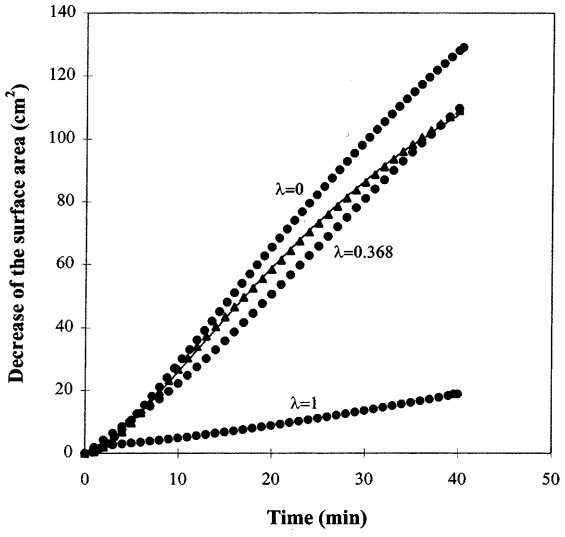

Fig. 8 Decrease in the surface area with time at $\pi = 5$ mN/m and pH 11.4 for a PLA50 ($M_w = 124\,400$) monolayer. Experimental data (*curve*); theoretical predictions of Eq. (13) together with Eqs. (9)–(11) with one fitting parameter k_0 and $\lambda = 0$, 0.368 and 1 (points) or with two fitting parameters k_0 and λ (*triangles*)

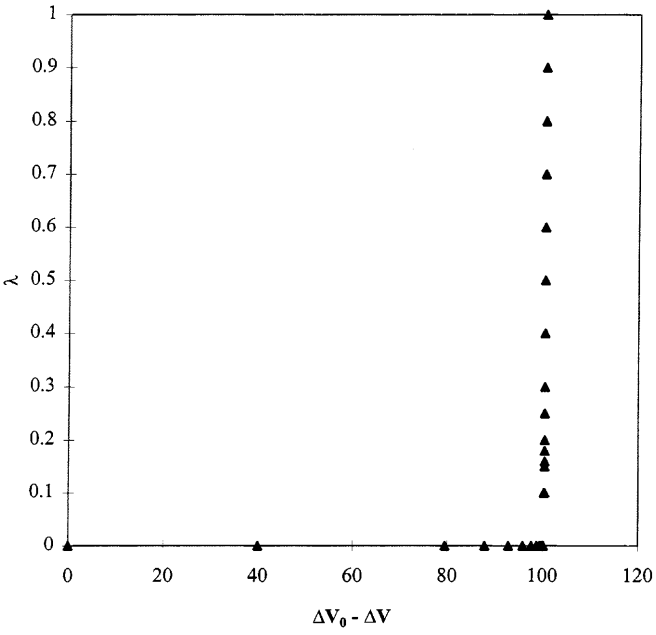

Fig. 9 Fitting parameter λ as a function of the electrostatic potential ($\psi_0 = \Delta V_0 - \Delta V$)

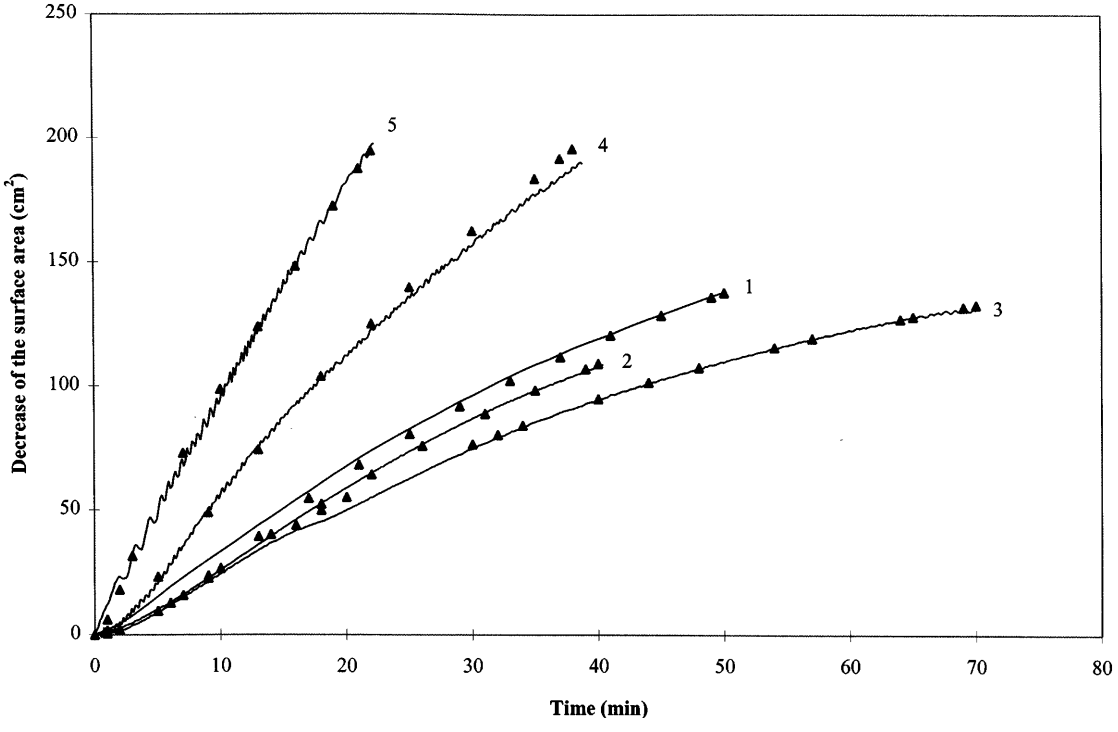

Fig. 10 Decrease in the surface area with time at $\pi = 5$ mN/m and pH 11.4 for PLA42.5GA15 ($M_w = 87\,000$) (*curve 1*); PLA50 ($M_w = 124\,400$) (*curve 2*); PLA50 ($M_w = 41\,600$) (*curve 3*); PLA25GA50 ($M_w = 102\,900$) (*curve 4*); PLA25GA50 ($M_w = 14\,300$) (*curve 5*). Experimental data (*curves*); theoretical predictions of Eq. (13) together with Eqs. (9)–(11) with two fitting parameters k_0 and λ (*triangles*)

From Eqs. (7) and (17), we obtain the following form of the Graham equation:

$$s^-(t) = \frac{1}{e_0}\sqrt{\frac{2n_+\varepsilon kT}{\pi}} \times \sinh\frac{e_0\left[\Delta V_0 - \Delta V(t) + 4\pi(\mu'_\perp - \mu_\perp)s^-\right]}{2kT}. \quad (18)$$

Table 1 Hydrolysis rate constant (k_0) at pH = 11.4 as a function of the surface pressure (π) for monolayers of poly(α-hydroxy acid)s

π (mN m^{-1})	k_0 (min^{-1})				
	PLA50 ($X_{LA/GA}$ = 1)		PLA42.5GA15 ($X_{LA/GA}$ = 0.85)	PLA25GA50 ($X_{LA/GA}$ = 0.5)	
	M = 41 600	M = 124 400	M = 87 000	M = 14 300	M = 102 900
2	0.024	0.018	0.025	0.075	0.070
3	0.021	–	0.035	0.088	0.070
5	0.034	0.030	0.039	0.130	0.065
10	0.042	0.030	0.035	0.100	0.046

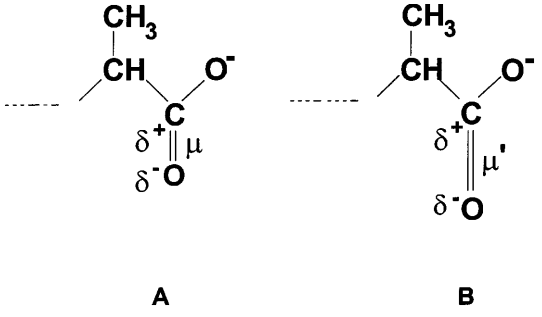

Fig. 11 Schematic representation of the modification of the positive dipole moment of carbonyl groups from $\mu_\perp$ (A) to $\mu'_\perp$(B)

The theoretical prediction of Eq. (14) for the accumulation of charged products $s^-(t)$ during hydrolysis based on surface-pressure measurements and the description of the processes of random fragmentation and solubilization is compared in Fig. 12 with the predictions of Eqs. (16) and (18) based on surface-potential measurements. The comparison shows that the results obtained by the two independent mechanical (Eq. 14) and electrical (Eq. 16) approaches are of the same order of magnitude. By using the more realistic expression (Eq. 18) with a reasonable value of $\mu_\perp = 159$ mD and the fitting parameter $\lambda(t)$, the two predictions are in good agreement.

In conclusion, both approaches, the mechanical one (detecting the progressive solubilization of small fragments) and the electrical one (detecting the progressive accumulation of charged insoluble products at the interface) confirm the ideas developed for the interfacial organization of hydrolysis in the framework of random

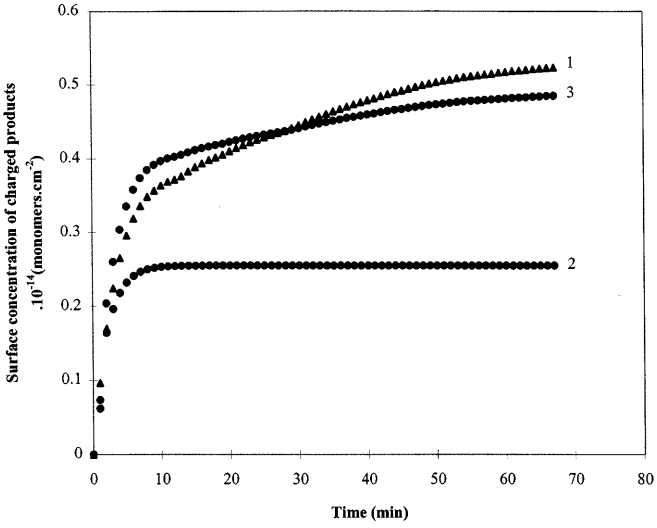

Fig. 12 Interfacial accumulation of negatively charged products during the hydrolysis of a PLA50 (M_w = 124 400) monolayer at π = 5 mN m^{-1} and pH 11.4, obtained from surface-pressure measurements and Eq. (14) (*curve 1*), surface-potential measurements and Eq. (16) (*curve 2*) and surface-potential measurements and Eq. (18) (*curve 3*)

scission hydrolysis. As well as the observed dependence of the hydrolysis rates on the length of the poly(α-hydroxy acid) polymers, we intend to test the role of end scission on the process of fragmentation in the future.

Acknowledgement This work was partially financed by the Bulgarian National Foundation for Scientific Research.

References

1. Vert M (1986) In: Buck S (ed) CRC critical reviews – Therapeutic drug carrier systems, vol 2. CRC Press, Boca Raton, p 291
2. Lewis DD (1990) In: Chasin M, Langer RS (eds) Biodegradable polymers as drug delivery systems. Dekker, New York, p 1
3. Mauduit J, Vert M (1993) STP Pharm Sci 3:197
4. Chu CC (1982) J Biomed Mater Res 16:117
5. Makino K, Arakawa M, Kondo T (1985) Chem Pharm Bull 33:1195
6. Makino K, Ohshima H, Kondo T (1986) J Microencapsul 3:203
7. Coffin MD, Mc Ginity W (1992) Pharm Res 9:200
8. Chu CC, Williams DF (1983) J Biomed Mater Res 17:1029
9. Koetsu I, Yoshida M, Asano M, Yamanaka H, Imai K, Yuasa H, Mashimo T, Suzuki K, Katakai R,

Oya M (1987) J Controlled Release 6:249
10. Vert M, Li S, Garreau H (1991) J Controlled Release 16:15
11. Fukuzaki H, Yoshida M, Asano M, Kumakura M, Mashimo T, Yuasa H, Imai K, Yamanaka H (1991) Biomaterials 12:433
12. Spenlehauer G, Vert M, Benoit JP, Boddaert A (1989) Biomaterials 10: 557
13. Shih C (1995) J Controlled Release 34:9
14. Batycky RP, Hanes J, Langer R, Edwards D (1997) J Pharm Sci 86:1464
15. Ivanova Tz, Panaiotov I, Boury F, Proust JE, Benoit JP, Verger R (1997) Colloids Surf B 8:217
16. Ivanova Tz, Panaiotov I, Boury F, Saulnier P, Proust JE, Verger R (1997) Colloids Surf B (in press)
17. Ringard – Lefebre C, Baszkin A (1994) Langmuir 10:2376
18. Davies JT, Rideal EK (1961) Interfacial phenomena. Academic Press, New York
19. Mac Ritchie F (1990) Chemistry at interfaces. Academic Press, San Diego
20. (a) Boury F, Olivier JE, Proust JE, Benoit JP (1993) J Colloid Interface Sci 160:1; (b) Boury F, Olivier JE, Proust JE, Benoit JP (1994) J Colloid Interface Sci 163:37
21. Boury F, Gulik A, Dedieu JC, Proust JE (1994) Langmuir 10:1654
22. (a) Boury F, Ivanova Tz, Panaiotov I, Proust JE, Bois A, Richou J (1995) J Colloid Interface Sci 169:380; (b) Boury F, Ivanova Tz, Panaiotov I, Proust JE, Bois A, Richou J (1995) Langmuir 11:1636